

Regimes of strong electrostatic collapse of a highly charged polyelectrolyte in a poor solvent.

Anvy Moly Tom,^{*a} Satyavani Vemparala,^a R Rajesh,^a and Nikolai Brilliantov^b

We perform extensive molecular dynamics simulations of a highly charged flexible polyelectrolyte (PE) chain in a poor solvent for the case when the chain is in a collapsed state and the electrostatic interactions, characterized by the reduced Bjerrum length ℓ_B , are strong. We detect the existence of several sub-regimes, $R_g \sim \ell_B^{-\gamma}$, in the dependence of the gyration radius of the chain R_g on ℓ_B . In contrast to a good solvent, the exponent γ for a poor solvent crucially depends on the size and valency of counterions. To explain the different sub-regimes we generalize the existing counterion fluctuation theory by a more complete account of the volume interactions in the free energy of the chain. These include interactions between the chain monomers, between monomers and counterions and the counterions themselves. We also demonstrate that the presence of the condensed counterions can modify the effective attraction among the chain monomers and impact the sign of the second virial coefficient.

1 Introduction.

Charged polymers in solution, or polyelectrolytes (PEs), are ubiquitous in nature and play a significant role in our everyday life. Common examples of PEs include biologically important molecules like DNA, RNA and proteins^{1–3}. PEs also find application in industries such as chemical^{4–7}, pharmaceutical^{8–11}, food^{12,13} etc. The mechanical and chemical properties of a PE depend on its conformational state, which could vary from being linear and extended to compact and collapsed. The conformational state is determined essentially by three properties: the strength of electrostatic interactions in the system, entropy of the counterions and quality of the solvent. Determining the precise role of these characteristic in the conformational state of a simple model PE is fundamental to understand the physics of more realistic PE systems.

The strength of the electrostatic interactions in the system depends on the charge density of the PE chain and is quantified by the reduced Bjerrum length ℓ_B

$$\ell_B = \frac{e^2}{\epsilon k_B T a} = \frac{\beta e^2}{\epsilon a}, \quad (1)$$

where ϵ is the dielectric permittivity of the solvent, k_B is the Boltzmann constant, T is temperature, $\beta = (k_B T)^{-1}$, and a is the distance between neighbouring charged monomers of the PE chain. ℓ_B quantifies the ratio of the electrostatic interaction energy between the neighbouring charged monomers and thermal energy. The larger the value of ℓ_B , the stronger the electrostatic interac-

tions in the system.

For small ℓ_B a PE behaves like a neutral polymer and the counterions are dispersed away from the PE to occupy all accessible volume, resulting in a state with high entropy. With increasing ℓ_B , the electrostatic interaction energy becomes comparable to the thermal energy and counterions begin to condense onto the PE, renormalizing its charge density¹⁴. The condensed counterions being in a close vicinity of the PE imply a lower entropy of the system. Still, if ℓ_B is not large, a PE conformation is dictated by the solvent quality.

The solvent quality, in turn, is determined by the relative strength of the attractive interactions between chain monomers and between monomers and solvent particles. In a good or theta-solvent these attractive interactions are stronger for monomer-solvent particle pairs, while in a poor solvent monomer-monomer attractive interactions dominate¹⁵.

Several experiments and simulations have shown that at large enough ℓ_B , like-charged PE chains undergo a transition from extended to collapsed conformations regardless of the solvent quality^{16–24}. This counterintuitive transition is driven by the condensation of counterions onto the chain, reducing the effective charge density. The nature of the effective attractive interactions driving the transition is not well understood and there are competing theories explaining their origin (see below). For the collapsed state, these theories predict that the gyration radius, R_g , of a PE has the scaling form $R_g \sim N^{1/3} \ell_B^{-\gamma}$, where N is the length of the PE, and the exponent γ can potentially depend on system parameters. Presently there exist three different theoretical approaches to explain this electrostatics-driven collapse in PEs^{19,25–30}. These theories differ from each other in the way the effective electrostatic interactions are modelled and lead to different predictions for the exponent γ . In the first approach it is argued that the free energy of a PE in a collapsed state corresponds to that of an amorphous ionic solid; this theory predicts a collapsed conformation for the case of multivalent counterions, with no dependence of R_g on ℓ_B ($\gamma = 0$)²⁷. In the second approach it is hypothesized that the freely rotating fluctuating dipoles formed between PE

^{0a} The Institute of Mathematical Sciences, C.I.T. Campus, Taramani, Chennai 600113, India

^{0b} Department of Mathematics, University of Leicester, Leicester LE1 7RH, United Kingdom

^{0†} Electronic Supplementary Information (ESI) available: [details of any supplementary information available should be included here]. See DOI: 10.1039/b000000x/

^{0‡} Additional footnotes to the title and authors can be included e.g. ‘Present address:’ or ‘These authors contributed equally to this work’ as above using the symbols: ‡, §, and ¶. Please place the appropriate symbol next to the author’s name and include a \footnotetext entry in the the correct place in the list.

monomers and condensed counterions give rise to an effective attractive interaction between segments of the chain, which causes a PE collapse both in good and poor solvents^{25,28–30}. This theory predicts that R_g of a PE in a collapsed state scales with Bjerrum length as $R_g \sim N^{1/3} |\ell_B^2 - cB_2|^{-1/3}$, where B_2 is the second virial coefficient, and c is a dimensional constant that depends on the details of the system^{25,29,30}. Hence for both good^{25,29,30} and poor^{25,30} solvents, γ is equal to $2/3$. In the third approach, known as counterion-fluctuation theory, it is argued that density fluctuations of condensed counterions inside a chain globule cause a negative pressure, which drives the PE collapse¹⁹. This theory predicts $\gamma = 1/2$.

In a recent molecular dynamics (MD) study of a flexible PE in a good solvent we showed that a collapsed PE conformation demonstrates at least two different sub-regimes, which we call as a weak electrostatic collapse, with $\gamma = 1/2$, and a strong electrostatic collapse with $\gamma = 1/5$. The exponent γ in both regimes was found to be independent of the valency of counterions and PE chain length³¹. All inter-particle interactions, other than electrostatic, were repulsive in these systems. The counterion-fluctuation theory, originally developed for good solvent with a single exponent $\gamma = 1/2$, has been generalized by us³¹ through the inclusion of higher order virial coefficients to reproduce both the weak ($\gamma = 1/2$) and strong ($\gamma = 1/5$) collapse regimes seen in our MD simulations.

It is more challenging however to study a collapsed state of a flexible PE in a poor solvent^{32–38} since, unlike in a good solvent, there exist additional attractive interactions between monomers which compete with the repulsive part of electrostatic interactions. The valency of counterions, which played no role in determining the exponent γ for a good solvent becomes significant for a poor solvent. Indeed, it dictates the number of counterions condensed inside the collapsed globule; the presence of the counterions modifies the overall interaction energy between the monomers due to the excluded volume interactions between all species and hence influences the exponent γ . In the present study, we report MD simulations for the collapsed phase of a strongly charged flexible PE in a poor solvent and find several novel collapse sub-regimes. The observed in MD simulations conformational behavior of a PE in a poor solvent can be explained by extending the modified counterion-fluctuation theory^{19,31} with a more complete account of the volume interactions between all species in the system: the monomer-monomer, monomer-counterion and counterion-counterion interactions. We show that the new theory can uniformly describe the MD results for both good and poor solvents.

The rest of the paper is organized as follows. In Sec. 2, we define the model and give details of the MD simulations. In Sec. 3, we present our theory of the electrostatic collapse in a poor solvent and compare the predictions with data from MD simulations. A summary and discussion of our results are given in Sec. 4.

2 Model and Methods

We model a flexible PE chain as N monomers of charge e connected by harmonic springs of energy

$$U_{bond}(r) = \frac{1}{2}k(r-a)^2, \quad (2)$$

where k is the spring constant, a is the equilibrium bond length, and r is the instantaneous distance between the bonded monomers. The PE chain and $N_c = N/Z$ neutralizing counterions with a valency Z are placed in a box of linear size L . Pairs of all non-bonded particles (counterions and monomers) separated by a distance r_{ij} interact through the volume (or van der Waals) interactions. Here we model these interactions by the Lennard Jones (LJ) 6 – 12 potential with a cutoff of r_c :

$$U_{LJ}(r_{ij}) = 4\epsilon_{LJ} \left[\left(\sigma/r_{ij} \right)^{12} - \left(\sigma/r_{ij} \right)^6 \right], \quad r_{ij} \leq r_c. \quad (3)$$

The values of ϵ_{LJ} and r_c are varied to model solvents of different quality (see below). The electrostatic energy between charges q_i and q_j separated by r_{ij} is given by

$$U_c(r_{ij}) = \frac{q_i q_j}{\epsilon r_{ij}}. \quad (4)$$

In the simulations, we use $a = 1.12\sigma$, $k = 500.0k_B T/\sigma^2$, $L = 370\sigma$, $N=204$. All energies are measured in units of $k_B T$, and we maintain temperature at 1 through a Nosé-Hoover thermostat. All distances are measured in terms of σ which we set to 1. The long-range Coulomb interactions are evaluated using particle-particle/particle-mesh (PPPM) technique.

The equations of motion are integrated in time using molecular dynamics simulation package LAMMPS³⁹ with a time step of 0.001. All the systems are equilibrated for 5×10^6 timesteps and the data presented in this paper are averaged over 5×10^6 timesteps of production runs.

We model a variety of poor solvent conditions by choosing the following combinations of the LJ energy parameters for ϵ_{LJ} and cutoff distance r_c for the monomer-monomer interactions: (i) $\epsilon_{LJ} = 1$ and $r_c = 2.5$, (ii) $\epsilon_{LJ} = 1.5$ and $r_c = 2.5$, and (iii) $\epsilon_{LJ} = 2$ and $r_c = 2.5$. For all other volume interactions among counterions and between monomers and counterions, the LJ interactions are repulsive, $\epsilon_{LJ} = 1.0$ and $r_c = 1.0$. These conditions are chosen in such a way, that when the charge on the monomers is zero, a PE chain adopts a collapsed conformation, mimicking poor solvent conditions. We also performed additional simulations in which the counterion size was varied. We note that all simulations reported in this paper have been performed for the values of ℓ_B , where the equilibrium configuration of a PE is a collapsed state with $R_g \sim N^{1/3}$.

3 Results

To develop a generalized theory for electrostatic-driven collapse of a PE in a poor solvent, we start with the modified counterion-fluctuation theory for a good solvent and retain the electrostatic term. As mentioned in the Introduction, the modified counterion fluctuation theory is able to explain the observed in MD simulations collapsed sub-regimes (with correct exponent γ) for a flex-

ible PE in a good solvent³¹. However, in the case of a poor solvent, we anticipate that the effective attraction between chain monomers, supplemented by attractive van der Waals forces, would cause even stronger collapse of a chain compared to that in a good solvent. In the following subsections, we generalize the theory of Ref.³¹ making a more complete account of the volume interactions and show that the counterion-fluctuation theory is applicable regardless of a solvent quality.

3.1 Free energy of a PE system

To find the equilibrium gyration radius R_g we compute the conditional free energy of the system $F(R_g)$ and minimize it with respect to R_g . We write the free energy of the system as a sum of its components as follows:

$$F(R_g) = F_{\text{id.ch}}(R_g) + F_{\text{en}}(R_g) + F_{\text{el}}(R_g) + F_{\text{vol}}(R_g), \quad (5)$$

where $F_{\text{id.ch}}$, F_{en} , F_{el} , and F_{vol} account for the free energy of an ideal chain, entropy of the counterions, the electrostatic interactions between the charged particles, and the volume interactions between all the species respectively.

$F_{\text{id.ch}}(R_g)$, the part of the free energy corresponding to the ideal chain reads^{15,19,40},

$$\beta F_{\text{id.ch}} \simeq \frac{9}{4} (\alpha^2 + \alpha^{-2}), \quad (6)$$

where $\alpha = R_g/R_{g,\text{id}}$ is the expansion factor, with $R_{g,\text{id}}$ being the gyration radius of the ideal chain, $R_{g,\text{id}}^2 = Na^2/6$.

The second part of the system free energy, $F_{\text{en}}(R_g)$ accounting for the entropy of the counterions is proportional to the logarithm of the volume available for the counterions. It may be shown that^{19,31},

$$\frac{\beta F_{\text{en}}}{N} = -\frac{3}{Z} (1 - \tilde{\rho}) \ln \left(\frac{R_0}{a} \right), \quad (7)$$

where $\tilde{\rho} = \rho_{\text{c.in}}/\rho_0$ with $\rho_{\text{c.in}}$ being the number density of counterions within the globule with the gyration volume $V_g = 4\pi R_g^3/3$ and $\rho_0 = N_c/V_g = N/(ZV_g)$ is the maximal counterion number density, when their condensation is complete. The value of R_0 refers to the volume $4\pi R_0^3/3$ per chain in the solution; it corresponds to L in our MD simulations.

The third part of the system free energy, $F_{\text{el}}(R_g)$, accounting for the electrostatic interactions among monomers and counterions is given by the counterion fluctuation theory¹⁹ as:

$$\frac{\beta F_{\text{el}}}{N} = \frac{3\sqrt{6}\ell_B N^{1/2} (1 - \tilde{\rho})^2}{5\alpha} \left(1 - \frac{2R_g}{3R_0} \right) - \frac{3}{2} \left(\frac{2}{\pi^2} \right)^{1/3} \frac{\ell_B \sqrt{6} Z^{2/3} \tilde{\rho}^{4/3}}{N^{1/6} \alpha}. \quad (8)$$

The first term in the right hand side of (8) gives the mean-field result for the electrostatic interactions in the system. The second term describes the contribution to the free energy from the correlated fluctuations of the charge density and is beyond the Poisson-Boltzmann approximation¹⁹. Both Eqs. (7) and (8) refer to dilute salt-free PE solutions of long chains, $R_0 \gg R_g$ and $N \gg 1$ ¹⁹.

Finally, the free energy $F_{\text{vol}}(R_g)$ accounting for the volume (LJ) interactions between monomers and counterions may be written

as

$$F_{\text{vol}}(R_g) = F_{\text{vol.m.m.}} + F_{\text{vol.c.m.}} + F_{\text{vol.c.c.}}, \quad (9)$$

where $F_{\text{vol.m.m.}}$, $F_{\text{vol.c.m.}}$, and $F_{\text{vol.c.c.}}$ are the free energy terms for the volume interactions between monomers, counterions and monomers, and between counterions respectively.

The monomer packing fractions, computed for the collapsed phase of the flexible PE in poor solvent considered here, vary from 0.1 to 0.25 across the range of electrostatic strengths considered here. Since the measured packing fractions are not too large¹⁵, we write the free energy as a virial expansion. Keeping up to the third virial term, we obtain for $F_{\text{vol.m.m.}}$:

$$\begin{aligned} \beta F_{\text{vol.m.m.}} &= (B_2 \rho_m^2 + B_3 \rho_m^3) V_g = \left(B_2 \left(\frac{N}{V_g} \right)^2 + B_3 \left(\frac{N}{V_g} \right)^3 \right) V_g \\ &= b^{-1} \frac{B_2}{\alpha^3 N^{1/2}} + b^{-2} \frac{B_3}{\alpha^6}, \end{aligned} \quad (10)$$

where B_2 and B_3 are the second and third virial coefficients for monomer-monomer interactions, $\rho_m = N/V_g$ is the average density of monomers inside the gyration volume and $b = (2\pi a^3/9\sqrt{6})$. For a collapsed state addressed here almost all counterions are located within the gyration volume of the chain. Then the average counterion density inside the gyration volume will be $\rho_{\text{c.in}} \simeq N_c/V_g = N/(ZV_g)$ and we neglect the counterion density outside this volume. The free energy of the volume interactions of the counterions will have the same form as in Eq. (10), but with the virial coefficients C_k for the counterion-counterion interactions, divided by Z^k , where Z is the valency of the counterions for the k -th virial term. A similar expression follows for the volume interactions between the chain monomers and counterions. Combining these expressions for $F_{\text{vol.m.m.}}$, $F_{\text{vol.c.m.}}$ and $F_{\text{vol.c.c.}}$ and limiting to third virial term, one arrives at the following result for the free energy F_{vol} for the case of complete counterion condensation:

$$\beta F_{\text{vol}} = \frac{\tilde{B}_2}{\alpha^3 N^{1/2}} + \frac{\tilde{B}_3}{\alpha^6}, \quad (11)$$

where \tilde{B}_2 and \tilde{B}_3 are the renormalized second and third virial coefficients respectively that account for all volume interactions. These coefficients read:

$$\tilde{B}_2 = b^{-1} \left(B_2 + \frac{2D_{1,1}}{Z} + \frac{C_2}{Z^2} \right) \quad (12)$$

$$\tilde{B}_3 = b^{-2} \left(B_3 + \frac{3D_{1,2}}{Z} + \frac{3D_{2,1}}{Z^2} + \frac{C_3}{Z^3} \right), \quad (13)$$

where C_k is k -th virial coefficient for the counterion-counterion interactions and $D_{l,k-l}$ are the virial coefficient for monomer-counterion volume interactions of l -th order with respect to the counterions and $(k-l)$ -th order with respect to monomers (see the Appendix for the detail). The value of the virial coefficients B_k , C_k and $D_{l,k-l}$ are determined by the relative strength of the LJ interactions and the thermal energy $k_B T$. Due to the dominance of repulsive forces in the monomer-counterion and counterion-counterion volume interactions considered here, all coefficients

C_k and $D_{l,k-l}$ are expected to be positive, $C_k > 0$ and $D_{l,k-l} > 0$ for $k \geq 2$ and $1 \leq l \leq k$. We also assume that the renormalized third virial coefficient \tilde{B}_3 is positive as well.

At the same time the sign of the renormalized second virial coefficient \tilde{B}_2 sensitively depends not only on its "bare" value B_2 (which is negative for poor solvents addressed here), but also on the counterion valency and the virial coefficients C_k and $D_{l,k-l}$, see Eq. (12). If these positive coefficients are large and the valency Z is small, \tilde{B}_2 becomes positive even for negative B_2 . Oppositely, for small C_k and $D_{l,k-l}$ and large Z the renormalized second virial coefficient remains negative, $\tilde{B}_2 < 0$. The values of the virial coefficients C_k and $D_{l,k-l}$ are determined by the size of counterions: The larger the counterions, the larger the virial coefficients. Hence it is expected that small counterions with a high valency imply negative \tilde{B}_2 , while large counterions with a low valency imply positive renormalized coefficient, $\tilde{B}_2 > 0$ (see the Appendix for the detail). This predictions will be checked in our MD simulations discussed below.

If the packing fraction of species (monomers and counterions) inside the gyration globule increases, the truncated expansion (10) loses its accuracy. One needs to use then an equation of state (EOS) for dense fluids, which may be the Flory-Huggins or van der Waals EOS with the appropriate parameters describing volume interactions. One can also use the EOS for Lennard-Jones mixtures, e.g.⁴¹. In the case of systems with larger packing fraction, additional terms in the virial expansion of (11) are included, which leads to the general form:

$$\beta F_{\text{vol}} = \sum_{k=2}^{\infty} \frac{N^{(3-k)/2}}{\alpha^{3(k-1)}} \tilde{B}_k, \quad (14)$$

that includes all the virial coefficients,

$$\tilde{B}_k = b^{1-k} \left(B_k + \sum_{l=0}^k \frac{\mathcal{C}_l^k}{Z^l} D_{l,k-l} + \frac{C_k}{Z^k} \right), \quad (15)$$

where $\mathcal{C}_l^k = k! / (l!(k-l)!)$ are the combinatorial coefficients, see the Appendix for the detail. Note that any non-singular EOS may be expressed in the form of Eq. (14), where the virial coefficient depend on the particular EOS. Here we use the approach developed for dense gases, where the virial coefficients are explicitly expressed in terms of the interaction potential⁴², see also the Appendix.

For small packing fractions only contribution from the first two terms, as in Eq. (11) is non-negligible. With the increasing density, next order virial terms in (14) start to play a role. It may happen that in some limited interval of packing fractions one particular term in the expansion (14) dominates. This will then manifest in a specific behavior of physical quantities for this interval (see the discussion below).

Combining the different contributions [Eqs. (6), (7), (8) and

(14)] the free energy in Eq. (5) attains the form,

$$\begin{aligned} \frac{\beta F(R_g)}{N} \simeq & \frac{9}{4N} (\alpha^2 + \alpha^{-2}) - \frac{3}{Z} (1 - \bar{\rho}) \ln \left(\frac{R_0}{a} \right) \\ & + \frac{3\sqrt{6}\ell_B N^{1/2} (1 - \bar{\rho})^2}{5\alpha} \left(1 - \frac{2R_g}{3R_0} \right) - \frac{\tilde{Z}^2 \ell_B}{N^{1/6} \alpha} + \sum_{k=2}^{\infty} \frac{N^{(1-k)/2}}{\alpha^{3(k-1)}} \tilde{B}_k, \end{aligned} \quad (16)$$

where $\tilde{Z}^2 = (3/2)(2/\pi^2)^{1/3} \sqrt{6} Z^{2/3}$.

In a collapsed state of a PE, addressed in the present study, almost all counterions are located inside the collapsed globule, regardless of the solvent quality, so that the average density of counterions is close to its maximal density inside the globule, $\rho_0 = N_c/V_g$. This suggests the approximation $\bar{\rho} \approx 1$, allowing us to ignore the second and third terms in the right hand side of Eq. (16). Moreover, since $R_g \sim N^{1/3}$ in a collapsed regime, the expansion factor $\alpha \sim N^{-1/6} \ll 1$. Thus, the term proportional to α^2 in $F_{\text{id.ch}}(\alpha)$ can be neglected. It is also straightforward to see that, in this limit, the term proportional to α^{-2} in $F_{\text{id.ch}}(\alpha)$ is small compared to the volume terms and may be dropped as well. With these approximations, Eq. (16) for the free energy of a PE in a collapsed state reduces to the following expression, regardless of the solvent quality:

$$\frac{\beta F}{N} = -\frac{\tilde{Z}^2 \ell_B}{N^{1/6} \alpha} + \sum_{k=2}^{\infty} \frac{N^{(1-k)/2}}{\alpha^{3(k-1)}} \tilde{B}_k. \quad (17)$$

3.2 Scaling of R_g and energies of a PE chain with ℓ_B

The dependence of gyration radius of a PE chain, $R_g = \alpha R_{g,\text{id}}$ on ℓ_B may be obtained by minimizing the free energy, Eq. (17), with respect to α , which results in,

$$\frac{\tilde{B}_2}{N^{1/3}} \alpha^{-2} + \frac{2\tilde{B}_3}{N^{5/6}} \alpha^{-5} + \frac{3\tilde{B}_4}{N^{4/3}} \alpha^{-8} + \dots = \frac{\tilde{Z}^2 \ell_B}{3}, \quad (18)$$

where a general term in the left-hand side of the above equation reads $(k-1)\tilde{B}_k N^{(4-3k)/6} \alpha^{4-3k}$. The relative importance of different terms in Eq. (18) depends on N , the virial coefficients \tilde{B}_k and the expansion factor α . In what follows, we show how the dominance of different virial terms in Eq. (18) gives rise to unique scaling exponents in the dependence of R_g on ℓ_B , for a limited interval of ℓ_B , that is, for a limited interval of species densities (monomers and counterions) inside the PE globule.

For the case of weak electrostatic collapse, the first term in the left hand side of Eq. (18) dominates yielding,

$$R_g = \frac{\sqrt{\tilde{B}_2} a N^{1/3}}{\sqrt{2\tilde{Z}} \ell_B^{1/2}}, \quad (19)$$

that is, $R_g \sim \ell_B^{-1/2}$. We note that this yields a meaningful result only if \tilde{B}_2 is positive. While this is trivially satisfied in the case of good solvent, for the poor solvent conditions considered here, the attractive LJ-forces between the monomers will prevail and the bare second virial coefficient B_2 is always negative, $B_2 < 0$. However as we show later the opposite condition $\tilde{B}_2 > 0$ may be satisfied even in the case of poor solvent for certain counterion sizes and valencies.

Table 1 The values of the exponent γ corresponding to the dominance of the k^{th} virial term.

k	γ
2	$1/2$
3	$1/5$
4	$1/8$
5	$1/11$
6	$1/14$
7	$1/17$
8	$1/20$
9	$1/23$

When ℓ_B increases and α becomes smaller, the subsequent terms in Eq. (18) begin to dominate over the first term. When the second or third terms on left hand side of Eq. (18) dominate, we obtain respectively the following exponents, $R_g \sim \ell_B^{-1/5}$ and $R_g \sim \ell_B^{-1/8}$:

$$R_g = \frac{\tilde{B}_3^{1/5} a N^{1/3}}{6^{3/10} \tilde{Z}^{2/5} \ell_B^{1/5}}, \quad (20)$$

and

$$R_g = \frac{\tilde{B}_4^{1/8} a N^{1/3}}{3^{1/4} \sqrt{2} \tilde{Z}^{1/4} \ell_B^{1/8}}. \quad (21)$$

In a general case, when the k -th virial term (with the coefficient \tilde{B}_k) dominates in some interval of ℓ_B , the gyration radius scales with the reduced Bjerrum length as $R_g \sim \ell_B^{1/(3k-4)}$. The sequence of the exponents γ for the inverse power of ℓ_B corresponding to k -th virial term is shown in Table 1.

We also derive the dependence of the internal energies, associated with the electrostatic and volume LJ interactions, on the gyration radius R_g . Using the thermodynamic relation for the internal energy $E = \partial \beta F / \partial \beta$, we obtain

$$\beta E_{el} / (N \ell_B) = -\tilde{Z}^2 a N^{1/3} / \sqrt{6} R_g \sim N^{1/3} R_g^{-1}, \quad (22)$$

$$\frac{\beta E_{LJ}}{N} = \frac{\tilde{B}_2' N}{R_g^3} + \frac{\tilde{B}_3' N^2}{R_g^6} + \frac{\tilde{B}_4' N^3}{R_g^9} + \frac{\tilde{B}_5' N^4}{R_g^{12}} + \dots, \quad (23)$$

where E_{el} and E_{LJ} are the electrostatic and LJ components of the internal energy and the constants \tilde{B}_k' may be expressed in terms of the temperature derivatives of the reduced virial coefficients \tilde{B}_k . These scaling laws can be easily measured in MD simulations.

3.3 MD results

To understand the effect of solvent quality on the scaling of R_g with ℓ_B , we have simulated a flexible PE in various poor solvents. In Fig. 1, we show the variation of R_g for a collapsed PE with ℓ_B for different counterion valency for two poor solvent conditions ($\epsilon_{LJ} = 1.0, 1.5$ and $r_c = 2.5$ for monomer-monomer interaction). In the case of $\epsilon_{LJ} = 1.0$ [see Fig. 1(a)–(c)], for all three valencies the weak and strong electrostatic collapse regimes with $\gamma = 1/2$ and $\gamma = 1/5$ are observed, when the compaction of the chain increases. However, in the case of divalent and trivalent counterions the additional sub-regimes appear, as ℓ_B further increases.

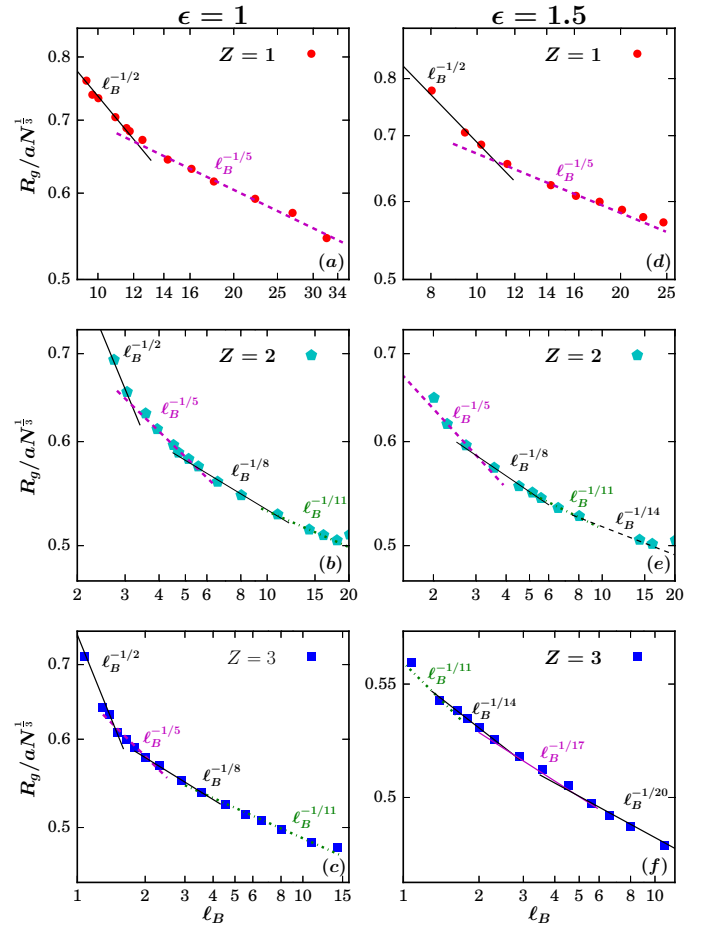


Fig. 1 Variation of the gyration radius R_g with ℓ_B for a PE chain with counterion valency $Z = 1$ (a,d); $Z = 2$ (b,e) and $Z = 3$ (c,f). The data are for poor solvent conditions ($\epsilon_{LJ} = 1.0$ and $\epsilon_{LJ} = 1.5$ and $r_c = 2.5$ for monomers). The solid straight lines correspond to power laws with exponents γ as predicted by the theory (see Table 1).

These regimes with smaller values of γ are observed for different intervals of ℓ_B , corresponding to the larger density of the PE globule. When ϵ_{LJ} is changed to 1.5 [see Fig. 1(d)–(f)], the weak electrostatic regime with $\gamma = 1/2$ persists only for monovalent counterions and vanishes for divalent and trivalent counterions. At the same time the regimes with smaller values of the exponent γ emerge. Corresponding data for $\epsilon_{LJ} = 2.0$ is given in Supplementary Information, where it is clearly demonstrated that the weak electrostatic regime with $\gamma = 1/2$ still persists for systems with monovalent counterions. The MD data presented in Fig. 1 are consistent with the theoretically predicted power laws. Both the values of the exponent γ and the sequence of their appearance are in agreement with the theory, see Table 1.

The appearance of $\gamma = 1/2$ for the poor solvent case shown in Fig. 1 is surprising since in poor solvent conditions, the second virial coefficient B_2 , when restricted to monomer-monomer interactions, is expected to be negative. Indeed, as we have mentioned above, if the charge of monomers is zero, the PE always adopts a collapsed state, corresponding to the negative value of B_2 ¹⁵. Then from Eqs. (19) and (20), it can be seen that the largest possible value for the exponent γ should be $1/5$, corresponding

to the (positive) third virial term. Hence we conclude that the presence of the counterions inside a collapsed globule leads to the change of the sign of B_2 for a certain range of LJ parameters and valency of counterions. This agrees with the above analysis, where we stated that for large counterions with a low valency the effective second virial coefficient \tilde{B}_2 is positive, although the bare coefficient B_2 is negative, yielding the regime with $\gamma = 1/2$. Physically, the negative sign of \tilde{B}_2 follows from the dominance of attractive volume interactions. Therefore, large counterions with a low valency (which implies the larger counterion density inside a globule) keep the chain monomers apart and reduce the effect of attractive volume interactions between them; this results in the alteration of the sign of \tilde{B}_2 . For $\tilde{B}_2 > 0$ the regime with $\gamma = 1/2$ is observed. At the same time small counterions of high valency (which implies lower density of these inside the globule) can not effectively keep the monomers apart, so that their attractive volume interactions yield a negative \tilde{B}_2 . For these systems the regime with $\gamma = 1/2$ is absent.

In other words, if the regime with $\gamma = 1/2$ is observed for some system ($\tilde{B}_2 > 0$), the decrease of a counterion size would entail the alteration of the sign of \tilde{B}_2 and hence disappearance of this regime, as for $\tilde{B}_2 < 0$. On the other hand, if the regime with $\gamma = 1/2$ is absent ($\tilde{B}_2 < 0$), the increase of the counterion size would lead to the change of the sign of \tilde{B}_2 and appearance of the regime with $\gamma = 1/2$, as for $\tilde{B}_2 > 0$.

To confirm these predictions, we perform additional simulations: Firstly, for the case of monovalent counterions we decrease the size of counterions and test whether the regime with $\gamma = 1/2$ disappears. Secondly, for the case of divalent counterions, we increase the size of counterions and check whether the regime with $\gamma = 1/2$ emerges. The MD data for these two simulations are shown in Fig. 2. In the case of monovalent counterions, as the size of the counterions is reduced, we find that the regime with $\gamma = 1/2$ vanishes [see Fig. 2(a)], that is, \tilde{B}_2 becomes negative, $\tilde{B}_2 < 0$. In the case of divalent counterions the regime with $\gamma = 1/2$, absent for $\sigma_c = 1$ [see Fig. 1(e)], appears when the counterion size increases up to $\sigma_c = 2$ [see Fig. 2(b)]. These data confirm that the presence of counterions inside the condensed phase modulates the effective attractive interactions between monomers and can change the sign of the second virial coefficient \tilde{B}_2 .

The counterion fluctuation theory, as developed in Sec 3.1, may be further substantiated by computing the energies E_{el} and E_{LJ} from MD simulations. As can be seen from Eq. (22), the scaling of E_{el} is independent of range of ℓ_B and solvent quality and scales as inverse of R_g . However, the dependence of E_{LJ} on R_g is more complicated ($E_{LJ} \sim R_g^{-3k}$) and is a function of dominant k -th virial term; this, in turn, depends on the range of ℓ_B , as can be seen from Eq. (23). The results for the scaling of E_{el} and E_{LJ} with R_g from our MD simulations are shown in Fig. 3. The data captures both the linear dependence of E_{el} on R_g and dependence of E_{LJ} on various powers of R_g very well, validating the free energy expression, Eq (17), obtained in the counterion fluctuation theory¹⁹. For E_{LJ} , we also note that as the valency of the counterions is increased, powers of R_g , corresponding to larger virial terms, appear. A possible physical explanation for this is that as the electrostatic interactions in the system become stronger and the pack-

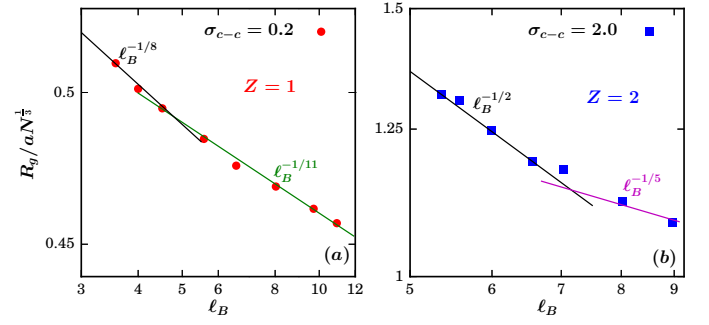


Fig. 2 (a) The disappearance of $R_g \sim \ell_B^{-1/2}$ and $R_g \sim \ell_B^{-1/5}$ regimes for monovalent-counterion system with $\varepsilon_{LJ} = 1$ by reducing the counterion radius [compare with Fig. 1(a)]. (b) The appearance of $R_g \sim \ell_B^{-1/2}$ regime for divalent-counterion system with $\varepsilon_{LJ} = 1.5$ by increasing the counterion radius [compare with Fig. 1(e)]. The chain length is $N = 204$.

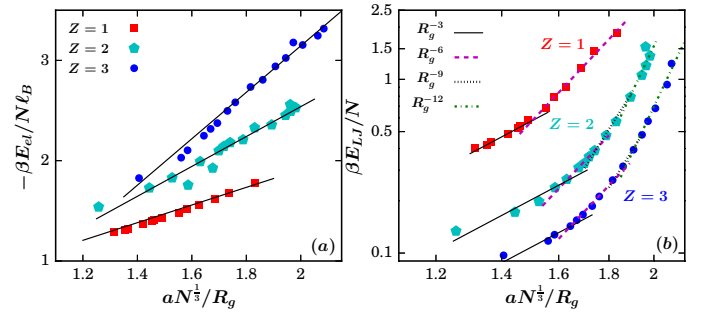


Fig. 3 The dependence of (a) the electrostatic energy E_{el} , (b) LJ energy E_{LJ} of the system on the gyration radius R_g for different valencies of counterions. $\varepsilon_{LJ} = 1.0$ and $r_C = 2.5$ for monomer-monomer interactions. The chain length is $N = 204$.

ing fraction of all species inside the globule increases, more terms to account for the volume interactions in the collapsed state are needed.

4 Discussion and conclusions

In this paper we studied theoretically and by means of MD simulations the nature of a collapsed state of a polyelectrolyte (PE) in a poor solvent for different strength of electrostatic and volume interactions. We detect several sub-regimes of the collapsed state of the PE, characterized by the scaling relation, $R_g \sim \ell_B^{-\gamma}$, for the gyration radius, R_g , and the reduced Bjerrum length, ℓ_B . From the MD simulations, we find that for different intervals of ℓ_B the exponent γ takes a series of values as a function of the solvent quality and the valency of counterions. This is consistent with the predictions of our theoretical analysis shown in Table 1. In particular, the exponent γ has a general form $\gamma = 1/(3k - 4)$, if in the part of the free energy, associated with the volume interactions, the k -th virial term dominates.

In our earlier work³¹ on collapsed regimes of a PE in good solvent, we had shown that modification of counterion-fluctuation theory¹⁹ can explain the scaling of R_g on ℓ_B observed in MD simulations. In the case of good solvent, for the values of ℓ_B studied, we detected only two sub-regimes: weak ($\gamma = 1/2$) and strong ($\gamma = 1/5$) electrostatic collapse, and the values of exponent were

found to be independent on the properties of the solvent and valency of the counterions. We explained the existence of these two regimes, modifying the existing counterion-fluctuation theory by inclusion of the third virial term into the volume part of the free energy of a PE. All volume interactions in this work were repulsive to emulate a good solvent; moreover all volume interactions were the same for monomers and counterions. In the current study, we further extend this formalism by explicitly considering the interactions between monomer-monomers, monomers-counterions and counterions-counterions and develop a generalized theory for a collapsed regime of a PE in any solvent. The good solvent case considered earlier is a special case of this generalized counterion-fluctuation theory.

We note that, while in MD simulations the solvent quality can be controlled by the interaction potential between monomers, in a theory this property is characterized by the sign of the second virial coefficient: B_2 is positive ($B_2 > 0$) for a good solvent and negative ($B_2 < 0$) for a poor one. It is not clear, however, whether this definition of solvent quality, based only on monomer-monomer interactions, remains meaningful for charged polymers in the presence of counterions. Within our generalized theory, we expect that the sign of the renormalized \tilde{B}_2 will be manifested in MD simulations through the presence of the sub-regime, $R_g \sim \ell_B^{-\gamma}$, with the exponent $\gamma = 1/2$ for $\tilde{B}_2 > 0$ and absence, respectively, of this regime for $\tilde{B}_2 < 0$.

In the current study, through extensive MD simulations, we demonstrate that the condensation of counterions on a PE chain leads to an effective renormalization of the volume virial coefficients. The renormalized virial coefficients strongly depend on the valency of counterions and the "strength" of the poor solvent, which may be characterized by the value of ε_{LJ} – the energy parameter of the LJ potential. Surprisingly, the MD results for a particular set of parameters for the volume interaction potential show, via the presence of sub-regime with the exponent $\gamma = 1/2$, that the renormalized second virial coefficient \tilde{B}_2 is positive. This is opposite to the expectation for this coefficient to be negative, as the simulations were performed for a poor solvent [see Fig. 1 (a)]. When the "strength" of the poor solvent ε_{LJ} increases, this sub-regime disappears for divalent and trivalent counterions but persists for monovalent counterions [see Fig. 1 (b)]. To understand the role of condensed counterions on the sign of renormalized \tilde{B}_2 , we performed a theoretical analysis as well as additional simulations in which we varied the size of counterions and demonstrated that the appearance and disappearance of sub-regime with $\gamma = 1/2$ crucially depends on the size of the counterions [see Fig. 2]. This dependence of the sign of the renormalized \tilde{B}_2 on counterion size and valency occurs only for a poor solvent, as the condensed counterions can modulate the effective attractive interactions between monomers resulting in the alteration of the sign of \tilde{B}_2 . For a good solvent, with repulsive interactions between the monomers, the counterion size and valency play no role, which may be clearly seen from Fig. 4, where we present the according results of MD simulations. The results in Fig. 4 combined with those in Fig. 2, show that while the sign of \tilde{B}_2 is unambiguous in a good solvent, the same is not true in the case of a poor solvent and depends on several system pa-

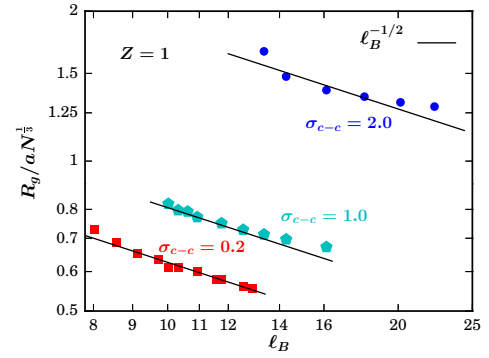


Fig. 4 The dependence of the gyration radius R_g for different radius of counterions for good solvent ($\varepsilon_{LJ} = 1$ and $r_c = 1$). The chain length is $N = 204$ and the valency of counterions $Z = 1$

rameters such as strength of the solvent, valency and size of the counterions. This suggests that for charged polymers with attractive monomer-monomer volume interactions and in the presence of counterions, the sign of the second virial coefficient cannot be assumed to be always negative. This is in a striking contrast with collapsed neutral polymers, which have the same attractive monomer-monomer interactions, where the sign of B_2 is always negative.

We also validate the predictions of the generalized counterion-fluctuation theory, developed in this paper, through the comparison of the theoretical and MD simulation results for scaling of different parts of the internal energy of the system with R_g . The original counterion-fluctuation theory¹⁹ predicts that the electrostatic internal energy of the system E_{el} scales with the gyration radius as $E_{el} \sim R_g^{-1}$ regardless of the sub-regime. At the same time, the dependence of internal energy associated with the volume (LJ) interactions is expected to be different for different sub-regimes, similar to the dependence of R_g on ℓ_B described above. From the theoretical analysis in we find that the LJ energy is expected to scale with R_g as $E_{LJ}(R_g) \sim R_g^{-3k}$, where k refers to the dominant k -th virial term in the part of the free energy that refers to the volume interactions. The MD simulation results are in complete agreement with these predictions [see Fig. 3]. We also note that the values of R_g at which the crossovers from one sub-regime of $E_{LJ}(R_g)$ to another take place [see Fig. 3] coincide with the values of R_g where the crossovers between regimes with different exponents γ are detected [see Fig. 1].

Based on our findings, we conclude that the effective attractive electrostatic interactions in systems of like-charged polymers in the presence of counterions is described well in terms of correlated fluctuations of counterions, as has been proposed in the counterion fluctuation theory¹⁹. The electrostatic term of the free energy of the system, based on the counterion fluctuation, is independent of the solvent quality. We note that none of the other existing theories of effective electrostatic interactions of a PE^{25,27–30} can explain the sequence of electrostatic sub-regimes or the scaling of the electrostatic energy with ℓ_B , as seen in our MD simulations.

5 Acknowledgments.

The simulations were carried out on the supercomputing machines Annapurna, Nandadevi and Satpura at the Institute of Mathematical Sciences.

6 Appendix

The free energy for the volume interactions among monomers may be written in the form of virial expansion as,

$$\begin{aligned}\beta F_{\text{vol.m.m.}} &= \sum_{k=2}^{\infty} B_k \rho_m^k V_g = \sum_{k=2}^{\infty} B_k \left(\frac{N}{V_g} \right)^k V_g \\ &= \sum_{k=2}^{\infty} \left(\frac{4\pi a^3}{3\sqrt{6}} \right)^{1-k} \frac{N^{(3-k)/2}}{\alpha^{3(k-1)}} B_k,\end{aligned}\quad (24)$$

where B_k is the k -th virial coefficient for monomer-monomer interactions and $\rho_m = N/V_g$ is the average density of monomers inside the gyration volume. Similar to Eq. (24), the free energy of the volume interactions of counterions reads,

$$\begin{aligned}\beta F_{\text{vol.c.c.}} &= \sum_{k=2}^{\infty} C_k \rho_{\text{c.in}}^k V_g = \sum_{k=2}^{\infty} C_k \left(\frac{N_c}{V_g} \right)^k V_g \\ &= \sum_{k=2}^{\infty} \left(\frac{4\pi a^3}{3\sqrt{6}} \right)^{1-k} \frac{C_k N^{(3-k)/2}}{Z^k \alpha^{3(k-1)}},\end{aligned}\quad (25)$$

where $\rho_{\text{c.in}} \simeq N_c/V_g = N/ZV_g$ is the average counterion density inside the gyration volume and we approximate it by the according density, when all counterions are condensed. C_k are the virial coefficients for the counterion-counterion interactions. Furthermore, the monomer-counterion volume interactions are described by the term,

$$\begin{aligned}\beta F_{\text{vol.c.m.}} &= \sum_{k=2}^{\infty} \sum_{l=0}^k \mathcal{C}_l^k \rho_c^l \rho_m^{k-l} D_{l,k-l} V_g \\ &= \sum_{k=2}^{\infty} \left(\frac{4\pi a^3}{3\sqrt{6}} \right)^{1-k} \frac{N^{(3-k)/2}}{\alpha^{3(k-1)}} \sum_{l=0}^k \frac{\mathcal{C}_l^k}{Z^l} D_{l,k-l},\end{aligned}\quad (26)$$

where $\mathcal{C}_l^k = k!/l!(k-l)!$ are the combinatorial coefficients and $D_{l,k-l}$ is the k -th virial coefficient for monomer-counterion volume interactions which refers to l counterions and $k-l$ monomers.

Using Eqs. (24), (25) and (26) one can write the part of the free energy responsible for the volume interactions in the system in the following compact form,

$$\beta F_{\text{vol}} = \sum_{k=2}^{\infty} \frac{N^{(3-k)/2}}{\alpha^{3(k-1)}} \tilde{B}_k, \quad (27)$$

where the renormalized virial coefficients \tilde{B}_k , that account for all volume interactions, are defined as

$$\tilde{B}_k = \left(\frac{2\pi a^3}{9\sqrt{6}} \right)^{1-k} \left(B_k + \sum_{l=0}^k \frac{\mathcal{C}_l^k}{Z^l} D_{l,k-l} + \frac{C_k}{Z^k} \right). \quad (28)$$

Here we consider a collapsed state of a PE chain and the main difference of a globular state, as compared to that of a coiled state is that a "globule contains a number of uncorrelated parts

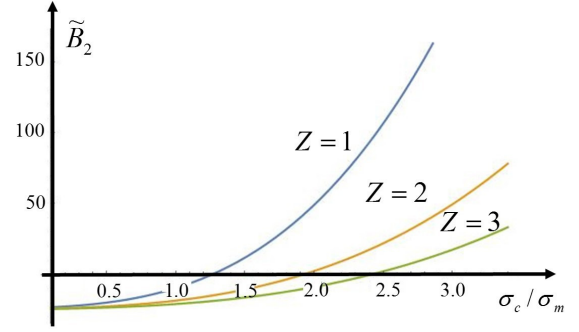


Fig. 5 The dependence of the renormalized second virial coefficient \tilde{B}_2 on the ratio of the counterion and monomer sizes, σ_c/σ_m and the counterions valency Z , as it follows from Eq. (12). The bare coefficients B_2 , C_2 and $D_{1,1}$ are computed using Eq. (29) with the according Lennard-Jones potentials: $\varepsilon_{LJ} = 1.5$ and $r_c = 2.5$ for the monomer-monomer interactions, $\varepsilon_{LJ} = 1$ and $r_c = 1$ for the counterion-counterion interactions and $\varepsilon_{LJ} = \sqrt{1} \cdot 1.5$ and $r_c = (2.5+1)/2 = 1.75$ for the monomer-counterion interactions. Depending on the valency of the counterions the renormalized coefficient \tilde{B}_2 changes its sign with the increasing size of the counterions.

of the chain" so that a concept of quasimonomers⁴³ and the according virial expansion for pressure or free energy is valid⁴⁰. In our study we use the LJ potential (3) to model all volume interactions. For the monomer-monomer interactions we use the cut-off distance $r_c = 2.5\sigma$, that is, these volume interactions include both attractive and repulsive forces. For the monomer-counterion and counterion-counterion interactions we use the cutoff $r_c = \sigma$, which corresponds to purely repulsive forces. The virial coefficient B_2 reads¹

$$\begin{aligned}B_2 &= -\frac{1}{2} \int d\mathbf{r} f(r) = -\int d\mathbf{r} \left(e^{-\beta U_{LJ}(r)} - 1 \right) \\ &= -2\pi \int_0^{r_c} dr r^2 \left(e^{-\beta U_{LJ}(r)} - 1 \right).\end{aligned}\quad (29)$$

Similar expressions apply for the coefficients C_2 and $D_{1,1}$, with the according change of the LJ potential. Using these expressions for the virial coefficients B_2 , C_2 and $D_{1,1}$ one can compute, using Eq. (12) the renormalized second virial coefficient \tilde{B}_2 . The results are presented in Fig. 5, where we demonstrate the dependence of \tilde{B}_2 on the size of the counterions σ_c and their valency Z . As it may be seen from the Fig. 5 the renormalized coefficient \tilde{B}_2 changes its sign from negative to positive with increasing size of counterions. This effect corresponds to an effective change of the solvent quality due to counterion condensation.

References

- 1 P. van der Schoot and R. Bruinsma, *Phys. Rev. E*, 2005, **71**, 061928.
- 2 V. A. Bloomfield, *Biopolymers*, 1991, **31**, 1471–1481.

¹ For simplicity we ignore the contribution to the second virial coefficient B_2 from the third virial coefficient B_3 that appears due to the chain connectivity⁴⁰. It may be shown that for the addressed range of parameters this contribution is positive and not large to yield a qualitative difference.

- 3 V. A. Bloomfield, *Curr. Opin. Struct. Biol.*, 1996, **6**, 334–341.
- 4 Q. Zhao, Q. F. An, Y. Ji, J. Qian and C. Gao, *J. Membr. Sci.*, 2011, **379**, 19–45.
- 5 H. Jiang, P. Taranekekar, J. Reynolds and K. Schanze, *Angew. Chem. Int. Ed.*, 2009, **48**, 4300–4316.
- 6 F. Renault, B. Sancey, P.-M. Badot and G. Crini, *Eur. Polym. J.*, 2009, **45**, 1337–1348.
- 7 J. Fang, X. Guo, S. Harada, T. Watari, K. Tanaka, H. Kita and K.-i. Okamoto, *Macromolecules*, 2002, **35**, 9022–9028.
- 8 B. G. De Geest, S. De Koker, G. B. Sukhorukov, O. Kreft, W. J. Parak, A. G. Skirtach, J. Demeester, S. C. De Smedt and W. E. Hennink, *Soft Matter*, 2009, **5**, 282–291.
- 9 S. Lankalapalli and V. M. Kolapalli, *Ind. J. Pharma. Sci.*, 2009, **71**, 481.
- 10 S. Shu, C. Sun, X. Zhang, Z. Wu, Z. Wang and C. Li, *Acta Biomater.*, 2010, **6**, 210–217.
- 11 S. Anandhakumar, M. Debapriya, V. Nagaraja and A. M. Raichur, *Mater. Sci. Eng. C*, 2011, **31**, 342–349.
- 12 E. Donath, G. B. Sukhorukov, F. Caruso, S. A. Davis and H. Möhwald, *Angew. Chem. Int. Ed.*, 1998, **37**, 2201–2205.
- 13 F. Shahidi, J. K. V. Arachchi and Y.-J. Jeon, *Trends. Food Sci. Technol.*, 1999, **10**, 37–51.
- 14 G. S. Manning, *J. Chem. Phys.*, 1969, **51**, 924–933.
- 15 A. Y. Grosberg and A. R. Khokhlov, *Statistical Physics of Macromolecules*, AIP Press, Woodbury, NY, 1994.
- 16 M. J. Stevens and K. Kremer, *Phys. Rev. Lett.*, 1993, **71**, 2228.
- 17 M. J. Stevens and K. Kremer, *J. Chem. Phys.*, 1995, **103**, 1669.
- 18 R. G. Winkler, M. Gold and P. Reineker, *Phys. Rev. Lett.*, 1998, **80**, 3731–3734.
- 19 N. V. Brilliantov, D. V. Kuznetsov and R. Klein, *Phys. Rev. Lett.*, 1998, **81**, 1433–1436.
- 20 S. M. Mel'nikov, M. O. Khan, B. Lindman and B. Jönsson, *J. Am. Chem. Soc.*, 1999, **121**, 1130–1136.
- 21 M. Deserno and C. Holm, *Mol. Phys.*, 2002, **100**, 2941–2956.
- 22 A. Varghese, S. Vemparala and R. Rajesh, *J. Chem. Phys.*, 2011, **135**, 154902.
- 23 A. V. Dobrynin and M. Rubinstein, *Prog. in Polym. Sci.*, 2005, **30**, 1049–1118.
- 24 A. A. Gavrilov, A. V. Chertovich and E. Y. Kramarenko, *Macromolecules*, 2016, **49**, 1103–1110.
- 25 H. Schiessel and P. Pincus, *Macromolecules*, 1998, **31**, 7953–7959.
- 26 R. Golestanian, M. Kardar and T. B. Liverpool, *Phys. Rev. Lett.*, 2016, **49**, 4456–4459.
- 27 F. J. Solis and O. de la Cruz, *J. Chem. Phys.*, 2000, **112**, 2030–2035.
- 28 A. Cherstvy, *J. Phys. Chem. B*, 2010, **114**, 5241–5249.
- 29 M. Muthukumar, *J. Chem. Phys.*, 2004, **120**, 9343–9350.
- 30 P. Kundu and A. Dua, *J. Stat. Mech.*, 2014, **2014**, P07023.
- 31 A. M. Tom, S. Vemparala, R. Rajesh and N. V. Brilliantov, *arXiv preprint arXiv:1606.02095*, 2016.
- 32 R. Chang and A. Yethiraj, *The Journal of Chemical Physics*, 2003, **118**, 6634D–6647.
- 33 U. Micka, C. Holm and K. Kremer, *Langmuir*, 1999, **15**, 4033–4044.
- 34 U. Micka and K. Kremer, *EPL (Europhysics Letters)*, 2000, **49**, 189.
- 35 N. Lee and D. Thirumalai, *Macromolecules*, 2001, **34**, 3446–3457.
- 36 R. Chang and A. Yethiraj, *Macromolecules*, 2006, **39**, 821–828.
- 37 H. J. Limbach and C. Holm, *The Journal of Physical Chemistry B*, 2003, **107**, 8041–8055.
- 38 P. Loh, G. R. Deen, D. Vollmer, K. Fischer, M. Schmidt, A. Kundagrami and M. Muthukumar, *Macromolecules*, 2008, **41**, 9352–9358.
- 39 S. Plimpton, *J. Comput. phys.*, 1995, **117**, 1–19.
- 40 A. Y. Grosberg and D. V. Kuznetsov, *Macromolecules*, 1992, **25**, 1970.
- 41 V. Harismiadis, A. Panagiotopoulos and D. Tassios, *Fluid Phase Equilibria*, 1994, **94**, 1.
- 42 C. A. Croxton, *Liquid state physics—a statistical mechanical introduction*, Cambridge University Press, London, 1974.
- 43 A. R. Khokhlov, *J. Phys.*, 1977, **38**, 845.